The 5th European sCO2 Conference for Energy Systems
March 14-16, 2023, Prague, Czech Republic

2023-sCO2.eu-106

# TRANSIENT SIMULATION AND ANALYSIS OF A SUPERCRITICAL $CO_2$ HEAT REMOVAL SYSTEM UNDER DIFFERENT ABNORMAL OPERATION CONDITIONS

**Markus Hofer***
University of Stuttgart
Stuttgart, Germany
Email: hofer@ike.uni-stuttgart.de

**Frieder Hecker**
Simulator Centre of KSG | GfS
Essen, Germany

**Michael Buck**
University of Stuttgart
Stuttgart, Germany

**Jörg Starflinger**
University of Stuttgart
Stuttgart, Germany

## ABSTRACT

The supercritical carbon dioxide ($sCO_2$[1]) heat removal system, which is based on multiple closed Brayton cycles with $sCO_2$ as the working fluid, is an innovative, self-propelling and modular heat removal system for existing and future nuclear power plants. Previous studies analysed its design, layout, control and operation. In addition, this novel study considers different sudden failures during the accident progress, e.g. failure of single $sCO_2$ cycles, control systems and valves. These abnormal conditions were investigated with the thermal-hydraulic system code ATHLET for a generic Konvoi pressurized water reactor. In most cases, the failure of a single $sCO_2$ cycle can be compensated. On the one hand, failure of the fans of the gas cooler leads to a pressure increase which may be mitigated by an inventory control system or cycle shutdown. On the other hand, unintended fan speed-up may cause compressor surge without adequate countermeasures. Furthermore, the system can operate under the cyclic blow-off from the steam generator safety valves when the relief valves are not available. Finally, the unintended closure of the valve which controls the steam flow through the compact heat exchanger triggers a fast cycle shutdown but a subsequent restart might be possible.

## INTRODUCTION

In case of a station blackout and loss of ultimate heat sink accident in a nuclear power plant, the plant accident management strongly depends on the recovery of electricity. If not available, core integrity will be violated, like in the Fukushima Daiichi accident. Such scenarios inspire the development of advanced decay heat removal systems. Since space is a limitation in existing power plants, the supercritical carbon dioxide decay heat removal system ($sCO_2$-DHRS) was proposed because of its compactness and self-propelling features [1,2]. Such a system could be incorporated into newly-built nuclear power plants as well as retrofitted to existing nuclear power plants. The system is not only self-propelling but its excess electricity can even be used to support other accident measures, e.g. recharging batteries. Moreover, no cooling water is required because the decay heat is transferred to the ambient air. To assess the benefits for nuclear safety, the $sCO_2$-DHRS needs to be analysed in detail.

Figure 1 shows the scheme of the $sCO_2$-DHRS attached to the steam generator (SG) of a pressurized water reactor (PWR). For better visualization, only one primary loop, which is connected to the pressurizer (PRZ), the corresponding steam generator (SG) and one attached $sCO_2$ cycle of the $sCO_2$-DHRS are displayed. In the case of a station blackout and loss of ultimate heat sink accident, the main coolant pumps stop and the containment is isolated. In the following, natural circulation develops on the primary side via the hot legs (HL), the u-tubes and cold legs (CL) and the heat is transferred to the secondary side of the steam generators (SG). Natural circulation also builds up on the secondary side of the steam generators via the compact heat exchangers (CHX) of the $sCO_2$-DHRS. After the start of the accident, all $sCO_2$ cycles are ramped up to their design heat removal capacity simultaneously. Later, when the decay power is lower than the total heat removal capacity, the operation of the cycles is adapted to the declining decay heat by control and successive shutdown of single cycles as shown later in Figure 2. In the CHX, the steam condenses and heats the $sCO_2$. The pressurized and heated $sCO_2$ is expanded in the turbine, which

[1] $sCO_2$ is defined as carbon dioxide at supercritical conditions with $p > 73.8$ bar and $T > 31$ °C

* corresponding author(s)



DOI: 10.17185/duepublico/77260

drives the compressor and generates power for the fans of the gas cooler (UHS). The compressor and the turbine are mounted on a common shaft together with the alternator and are referred to as turbo-alternator-compressor (TAC) or turbomachinery. After the turbine, the remaining heat of the $sCO_2$ is removed in the gas cooler to the ambient air, which serves as the diverse ultimate heat sink. For simplicity, the heat exchanger to the diverse ultimate heat sink will be called "UHS" in the following. Finally, the $sCO_2$ is compressed and flows to the CHX. Similarly, the $sCO_2$-DHRS can be directly attached to the reactor pressure vessel (RPV) of a boiling water reactor [1].

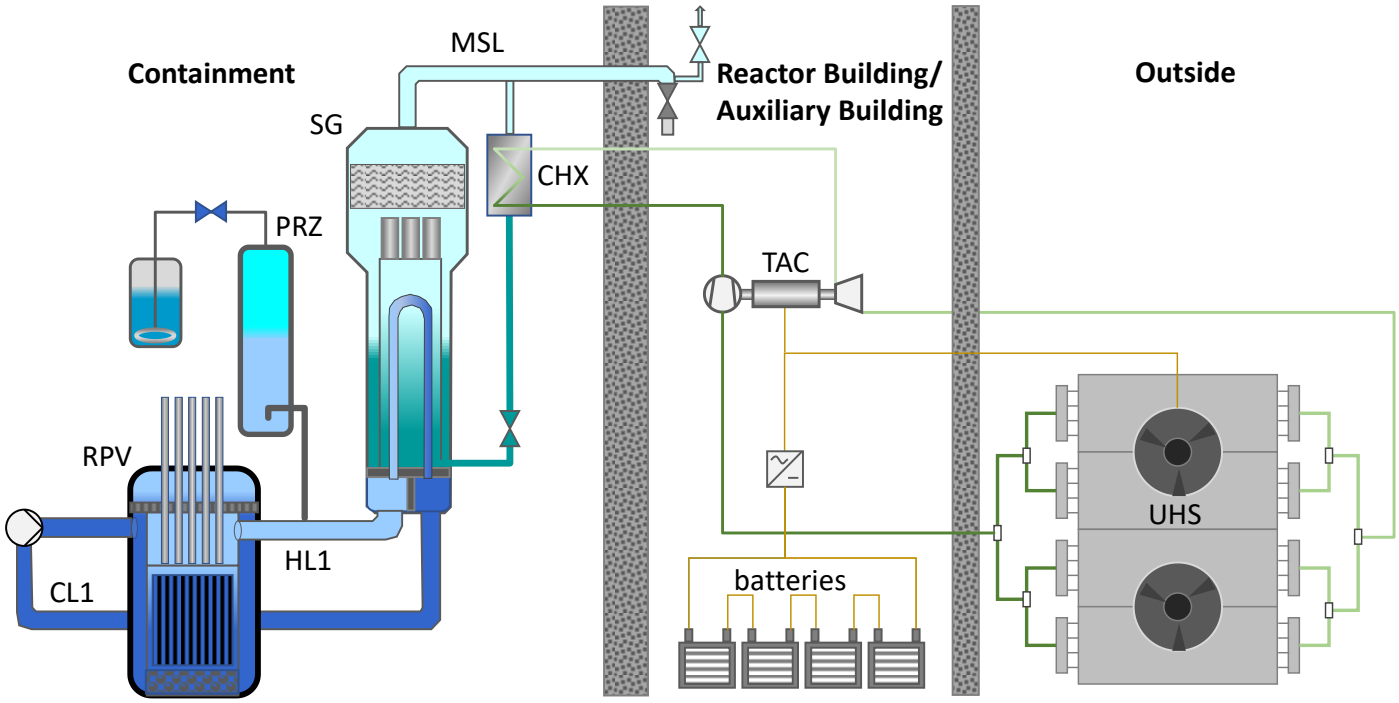


**Figure 1:** The $sCO_2$ heat removal system attached to the steam generator (SG) of a pressurized water reactor (PWR)

A comprehensive review of all kinds of $sCO_2$ power generation applications as well as cycle, component and control aspects was given by White et al. [1]. Wu et al. [2] provided an extensive review of the $sCO_2$ Brayton cycle for nuclear applications, considering experimental and numerical work, the application as a power conversion system as well as a heat removal system. Among other things, they highlight the need for further safety analysis and dynamic simulations. The safety and thermal-hydraulics of water-cooled nuclear power plants are discussed in detail by D'Auria et al. [3]. For the simulation of the thermo-hydraulic behaviour, different system codes are used, e.g. CATHARE, RELAP, TRACE, ATHLET, SCTRAN and SAS4A/SASSYS-1 [3–6]. Because $sCO_2$ is considered a working fluid for 4th generation reactor concepts as well as for the proposed heat removal system, work is in progress to extend or couple these system codes for the simulation of $sCO_2$ power cycles [5–13].

The thermal-hydraulic system code ATHLET [4,14,15], which is used for this study, is applied to analyse the whole spectrum of leaks and transients in nuclear power plants of Generation II-IV as well as Small Modular Reactors. The highly modular code structure of ATHLET includes advanced thermal-hydraulics as well as physical and numerical models. The main modules are thermo-fluid dynamics, heat transfer and heat conduction, neutron kinetics, control and balance-of-plant and the numerical time integration method. For a detailed study of the code features, the ATHLET "Models and Methods" manual [14] can be used. Bestion [4] compares different thermal-hydraulic system codes, regarding their models, capabilities and limitations. A short introduction to ATHLET is provided in [7,16].

Venker [7] investigated the $sCO_2$-DHRS for a boiling water reactor in detail by implementing first extensions for the simulation of the heat removal system in ATHLET. The successive shutdown of single cycles enabled the decay heat removal for more than 72 h. However, the component models, design and control of this system should be improved and different ambient temperatures and decay heat curves need to be considered in the future. Within the project sCO2-HeRo, Hajek et al. [17] and Vojacek et al. [18] described the basic principles for the integration of the $sCO_2$-DHRS into the European PWR fleet including safety, reliability and thermodynamic design considerations and first simulations with Modelica. As part of the project sCO2-4-NPP, the validation status for modelling $sCO_2$


DOI: 10.17185/duepublico/77260

cycles was provided for the codes CATHARE, Modelica and ATHLET including a blind benchmark [12]. Successful simulations were performed but it was also found that component models need further improvement and some numerical issues need to be solved in the future. Hofer et al. [11] presented improved models for ATHLET, including heat exchanger and turbomachinery models. The turbomachinery models are performance map based and use a real gas similarity approach [19] to account for changes in the inlet conditions. They also provided a design approach for the $sCO_2$-DHRS and analysed the $sCO_2$ cycle with varying decay heat [20] and at different ambient temperatures [16,21]. The cycle was successfully operated in part-load by adapting the rotational speed of the turbomachinery, keeping the compressor inlet temperature constant and without the need for inventory control. In [16,21], the modelling and design were improved, including new $sCO_2$ turbomachinery performance maps [22] with a higher surge margin, and the start-up from an operational readiness state was considered. Using Modelica coupled with ATHLET, Frýbort et al. [23] presented a first analysis of the challenging push-start from shutdown conditions and an alternative control strategy for low ambient temperatures, which is a combination of inventory control and UHS bypassing. Future analysis is required to analyse the feasibility of the push start, e.g. start at low ambient temperatures or determination of an appropriate heating procedure. The $sCO_2$-DHRS was integrated and simulated coupled to an EPR, VVER 1000 and Konvoi PWR with CATHARE, ATHLET/Modelica and ATHLET, respectively [16,24,25]. In all power plants, the same modular $sCO_2$-DHRS with a heat removal capacity of 10 MW per $sCO_2$ cycle was installed and successful coupled simulations with different numbers of systems were performed.

In the field of $sCO_2$ cycles for power generation, various dynamic analyses were conducted considering normal operation as well as failure conditions. Despite the focus on power generation, many findings are also relevant for the considered heat removal system. Hexemer et. al. [10,26] presented a detailed TRACE model of a recuperated $sCO_2$ cycle with two turbines. They highlighted the importance of performing a detailed transient analysis before the system design is finalized. Moreover, attention is drawn to the problem of compressor surge and turbine flow reversal. Nathan [27] investigated control strategies for an indirect $sCO_2$ recompression cycle. The major control strategies are high and low-temperature control, turbine bypass, and inventory control. These strategies enable successful cycle operation for different transients, like start-up and shutdown, part-load operation, loss-of-load, loss of heat sink and over-power. Moisseytsev and Sienicki [28] performed extensive steady-state and transient studies with the Plant Dynamics Code, including validation with data from Sandia National Laboratories and the $sCO_2$ Integrated System Test facility. Moreover, the Plant Dynamics Code was coupled to SAS4A/SASSYS-1, e.g. to analyse a wide range of thermal transients in the sodium-$CO_2$ reactor heat exchanger. For normal operation, design-basis accidents and severe accidents, the maximum gradient of the wall temperature was 0.2 K/s, 1 K/s, 2 K/s, respectively [29]. Wang et al. [30] highlighted the importance of failure analysis and analysed the loss of heat source, loss of cooling water and pipeline leakage for a recompression $sCO_2$ cycle and presented emergency measures to mitigate these failure conditions. Fast intervention was required in the last two scenarios to prevent system damage, e.g. discharging $CO_2$ after the loss of cooling water to avoid over-pressure.

This study presents the first analysis of various failures during the operation of the $sCO_2$-DHRS coupled with a generic Konvoi PWR. The design, layout and control of the applied $sCO_2$ cycle and the integration into the Konvoi PWR have already been discussed shortly in this chapter and can be found in detail in [21,24]. Furthermore, the applied models and their validation with data from small-scale experimental facilities were provided in [11,12,22].

In this paper, firstly, the normal operation and the operation strategy of the sCO2-DHRS are revisited also considering the failure of a $sCO_2$ cycle. Secondly, the failure of the fans (loss of cooling) of one cycle is analysed. Thirdly, the consequences of an unintended speed-up of the fans are presented including the effect of a fast intervention. Fourthly, the behaviour of the sCO2-DHRS during the cyclic blow-off from the steam generator safety valves is analysed. Finally, failures in the control of the steam flow through the CHX are investigated including a fast cycle shutdown and a subsequent restart.

Overall, the ATHLET simulations show that the $sCO_2$-DHRS can cope with some of these events but other cases either require fast intervention or further design or control improvements.

## NORMAL OPERATION AND FAILURE OF A SINGLE SCO2 CYCLE

In this chapter, the normal operation of the $sCO_2$-DHRS is discussed in comparison to the operation after the failure of one $sCO_2$ cycle. All simulations in this and the following chapters were performed with a $sCO_2$-DHRS consisting of four $sCO_2$ cycles coupled to a generic Konvoi PWR with a thermal power of 3840 MW considering a long-term station blackout and loss of ultimate heat sink scenario. With respect to the $sCO_2$ cycles, three process parameters were controlled: the compressor inlet temperature via the fan speed of UHS, the balance of decay heat and heat removal by controlling the turbine inlet temperature via the shaft speed of the turbomachinery and the CHX outlet temperature on the $H_2O$ side via the corresponding valve (Figure 1). If not stated otherwise, all simulations were conducted at the highest ambient temperature, which is 45 °C. Additionally, a conservatively low decay heat curve was applied in this chapter because this requires the highest operational flexibility from the $sCO_2$-DHRS [24].

Firstly, the normal operation and the operation strategy of the $sCO_2$-DHRS are revisited. On the left side of Figure 2, the decay power and the total thermal power removed by the $sCO_2$ cycles are shown. On the right side, the shaft speed of all four $sCO_2$ cycles is displayed. Solid lines mark the normal operation and dotted lines the operation after the failure of cycle 3, which


DOI: 10.17185/duepublico/77260

is discussed later. After the start of the accident, the $sCO_2$-DHRS is ramped up to its design shaft speed and design thermal power to reduce the steam blown down via the relief valves of the steam generators. Then, the shaft speed is kept constant until the turbine inlet temperature of the $sCO_2$ cycle has decreased to 260 °C. This temperature decrease on the NPP and $sCO_2$ side starts after the decay power has dropped below the removed thermal power. In the following, the shaft speed is controlled to keep the turbine inlet temperature constant. The limit of 260 °C was selected to ensure a sufficiently high turbine inlet temperature and to keep the primary circuit in a hot state to avoid reactivity increase and hence the need for early boron injection on the NPP side. To further ensure a sufficient thermal power input to the $sCO_2$ cycles, single cycles are shut down successively after 3.8 h, 9.3 h and 25.9 h, respectively. After each shutdown, the control increases the shaft speed of the remaining cycles automatically to match the decay power again. Altogether, this allows a smooth operation along the decay heat curve.

Secondly, the failure of a single cycle after the equilibrium of decay power and the removed power is discussed to justify the shutdown strategy of the $sCO_2$ cycles. In the simulation, relative switch-off speeds in relation to the cycle design point speed of 50 %, 35 % and 30 % were specified for the first, second and third cycles, respectively. The switch-off speeds were selected relatively low to be able to buffer the sudden failure of another operating cycle. The sudden failure of cycle 3 is exemplarily shown in Figure 2 concurrently with the second shutdown at around 9.3 h, indicated by the dotted lines. As a result, the removed thermal power drops to a lower value but the shaft speed control easily adapts the operation of the remaining cycle 4 to match the decay heat curve again. Thus, a cycle failure can normally be buffered by the remaining cycles. However, additional backup cycles should be installed to cover the unavailability of one or multiple cycles due to failures or maintenance, especially in the early phase of the accident. The next chapter provides an example of reduced heat removal after only 5 h and the last chapter before the conclusion considers a cycle failure after only 2 h. Additionally, the progress of the accident with only two or three available $sCO_2$ cycles can be found in [24]. Two cycles are not sufficient to handle the accident from the start and with three cycles the danger of recriticality may occur and the core is almost uncovered.

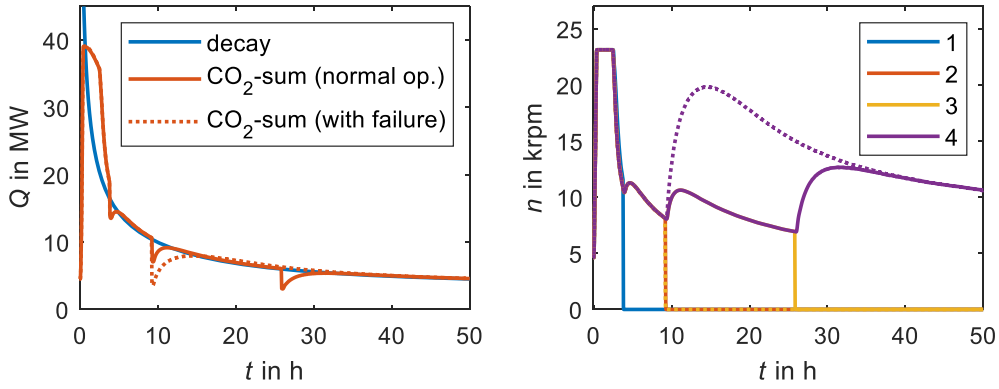


**Figure 2:** Normal operation (solid lines) vs. failure of cycle 3 concurrent with the shutdown of cycle 2 (dotted lines): decay power and total power removed by the $sCO_2$ cycles (left); shaft speed of turbomachinery for each of the four cycles (right)

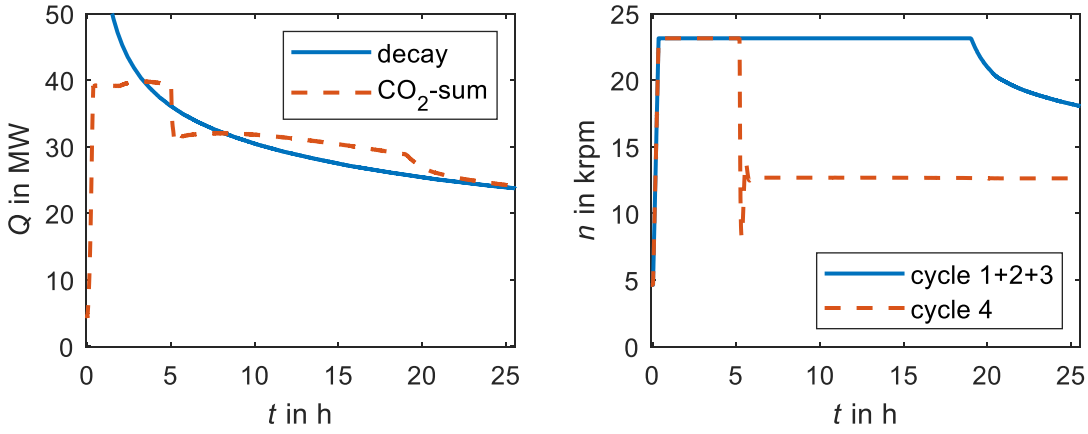


**Figure 3:** Fan failure of cycle 4: decay power and total power removed by the $sCO_2$ cycles (left); shaft speed of turbomachinery for each cycle (right)


DOI: 10.17185/duepublico/77260

## FAN FAILURE

In this chapter, the complete failure of the fans of the UHS of one $sCO_2$ cycle is analysed. It was assumed arbitrarily that the failure occurs 5 h after the start of the accident. In this case, a conservatively high decay heat curve was applied to highlight the effect of reduced heat removal [24]. Four $sCO_2$ cycles were under operation and the fan failure was considered in cycle 4. After the fan failure, a natural convection-driven air flow rate provided a small cooling power to the $sCO_2$ cycle. Under these conditions the assumed air mass flow rate was 3 % of its design flow rate [38].

On the left of Figure 3, the decay power compared to the total thermal power removed by all $sCO_2$ cycles is shown. The first 5 h are identical to the analysis in [24] and qualitatively similar to the previous chapter. Then, as a result of the fan failure, the removed thermal power drops from 39.3 MW to 30.8 MW, initially, and increases to 32 MW again. The reason for this behaviour is mainly related to the fact that cycle 4 is not switched off but continues to operate at reduced shaft speed, as can be observed in Figure 3 on the right. Since the total thermal power consumption of the $sCO_2$ cycles drops below the decay heat curve, the primary and secondary sides of the NPP start to heat up again but no additional mass is lost because the pressures stay below the set point of the valves. After 8.2 h, the equilibrium of the decay power and the removed thermal power is reached again and the temperatures and pressures start to decrease again until the shaft speed control adapts the removed thermal power to the decay power. Cycles 1 to 3 operate identically, therefore, these cycles are represented by a single line in this and the next figure.

In the following, some consequences of the fan failure are analysed in more detail. Figure 4 displays the compressor inlet temperature $T_{comp,in}$ and the turbine inlet temperature $T_{turb,in}$. $T_{comp,in}$ increases steeply after the fan failure because the cooling capacity of the UHS is reduced significantly. First, this also leads to an increase of $T_{turb,in}$ but then $T_{turb,in}$ decreases steeply to almost 250 °C. This is related to the control of the $H_2O$ outlet temperature of the CHX attempting to keep the condensate temperature at 150 °C by closing the control valve, hence blocking the water-steam flow through the CHX. When $T_{turb,in}$ drops below its target value of 260 °C, the shaft speed control is activated and decreases the shaft speed to increase $T_{turb,in}$ to its target value again. After approximately 45 min, the control succeeds at about half the nominal speed, and $T_{turb,in}$ stays constant at 260 °C and also $T_{comp,in}$ stabilizes at a value of 142.5 °C. In the other $sCO_2$ cycles, $T_{comp,in}$ is controlled to its target value of 55 °C and $T_{turb,in}$ follows the behaviour of the corresponding secondary steam temperature.

After the transient, the thermal power of the CHX of cycle 4 stabilizes at 2 MW together with an electrical power consumption of the turbomachinery of only 0.03 MW, which can be provided easily from the excess power of the other cycles.

It should be noted, that due to the constant mass inventory of the $sCO_2$ cycle, the considerably increased temperatures on the low-pressure side of cycle 4, lead to significantly higher cycle pressures. After the operation of cycle 4 stabilized again, the compressor inlet pressure is at 25.2 MPa and the outlet pressure at 27.2 MPa. Compared to the design values of the cycle, these values are 12.6 MPa and 5.8 MPa higher, respectively. If a constant mass inventory is also considered in future analysis, the pipe and component design have to take the higher pressures into account. An alternative may be an additional inventory control system. However, this would increase the complexity of the system and the required $sCO_2$ storage tank has to be quite large due to the large volume of the low-pressure side. Generally, it should be noted that the operation of the $sCO_2$ cycle might be quite unstable due to changes in the natural convection-driven airflow, which was assumed constant in the simulation. Therefore, another option is the intentional shutdown of the cycle affected by the fan failure and a later restart.

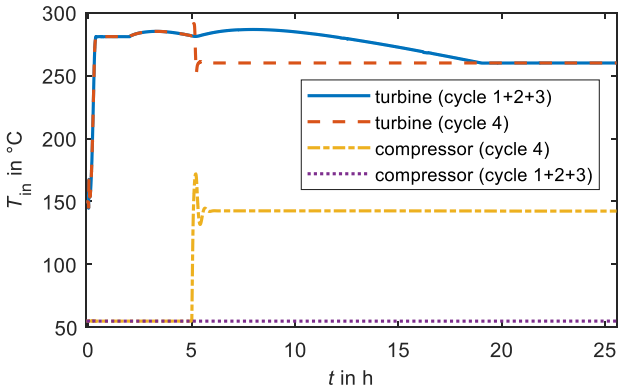


**Figure 4:** Fan failure of cycle 4: Compressor inlet temperature and turbine inlet temperature for each cycle

## UNINTENDED FAN SPEED UP

This chapter discusses the unintended speed-up of the fans, e.g. due to a failure of their control. Normally, the fan speed of the UHS is controlled to keep the compressor inlet temperature constant at its design value of 55 °C. However, in this case, it was assumed that the fan speed increased within 5 s to its design speed, due to a defect in the control system, 5 h after the start of the accident. In contrast to the other analyses, which considered an ambient temperature of +45 °C, this analysis was conducted at the lowest considered ambient temperature of –45°C because the sensitivity of the cycle to changes in the fan speed is increasing with decreasing ambient temperature. To lessen this increase in sensitivity to a certain extent, the heat transfer area of the UHS is reduced by disconnecting UHS modules from the cycle. At the assumed ambient temperature, only one quarter of the UHS was in operation.

As a result of the fan speed up, the air flow rate and cooling power are increasing and the cycle temperatures are decreasing steeply together with the cycle pressures due to the constant mass inventory. Since the active turbomachinery shaft speed control tries to keep the turbine inlet temperature constant, the shaft speed also decreases rapidly. After 20 s, the compressor inlet


DOI: 10.17185/duepublico/77260

temperature, pressure and mass flow rate already decreased by 15 K, 3 MPa and 2.5 kg/s, and the compressor operating point considerably approached the surge line. Around 30 s later, the compressor inlet drops below the critical pressure into the two-phase region and the simulation stops, since no subcritical $CO_2$ properties were implemented. At this point, the implemented turbomachinery control already decreased the shaft speed and the cycle mass flow rate to less than 30 % of the design shaft speed and 8.5 kg/s, respectively. At the end of the simulation, the theoretical surge line is almost crossed.

A further simulation analysed the effects of a fast intervention. The fan speed was increased within 5 s to its design value, as in the previous simulation. Then, the speed was decreased to its initial value within the same time and, finally, the speed control took over again. All other boundary conditions are identical to the previous simulation. On the left of Figure 5, the air mass flow rate visualizes the shaft speed increase and the following decrease and the resulting compressor inlet temperature is displayed with the start of the fan speed-up shifted to $t = 0$. This temperature shows an oscillation between 50.5 °C and 57 °C and after approximately 200 s the specified target value of 55 °C is reached again. Since the different conditions in the cycle are related, almost all parameters show similar oscillations, e.g. the magnitude of the compressor inlet pressure variation is 1 MPa and the cycle mass flow rate varies by 1.1 kg/s, which is also shown in Figure 5 on the right. Therefore, if the fan speed increase is stopped and decreased again to its initial value in time, this will only shortly affect the operation of the $sCO_2$ cycle.

It can be concluded that such an event requires a fast intervention or rather additional safety procedures, e.g. an upper limit for the fan speed relative to its current operation point. At least compressor surge can also be avoided by the opening of the turbine bypass or the compressor recirculation.

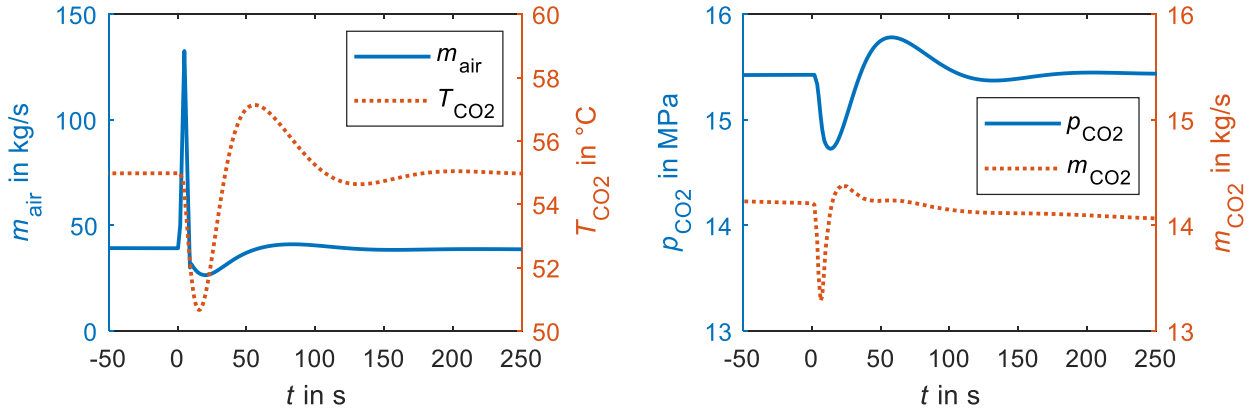


**Figure 5:** Fan control failure of cycle 4 (with intervention); $t = 0$ marks the start of the fan speed-up: Air mass flow rate and compressor inlet temperature (left); pressure and mass flow rate at the compressor inlet (right)

## CYCLIC BLOW-OFF FROM THE STEAM GENERATOR SAFETY VALVES

In this chapter, the steam generators are blown down via the safety valves instead of considering the partial depressurization to 7.5 MPa via the diverse blow-off valves. This might occur if the batteries of the diverse blow-off valves are not available or if the control of these valves does not work as intended. The simulation was conducted with the conservatively high decay heat curve since this results in an increased blowdown via the safety valves.

In terms of the long-term behaviour, after the blow-off has stopped, this simulation is very similar to the simulation with active diverse blow-off valves and partial depressurization to 7.5 MPa. After 3.1 h, the equilibrium of the decay power and the total thermal power of all $sCO_2$ cycles is reached and the shaft speed control adapts the thermal power of the $CO_2$ cycles to the decay power.

In the following, the transient behaviour of the $sCO_2$ cycles during the blow-off via the safety valves is analysed. Therefore, only the first 3 h of the accident are shown. All $sCO_2$ cycles and steam generators behave equally. Thus, some parameters of the CHX attached to steam generator 1 and of $sCO_2$ cycle 1 are shown. Figure 6 presents the temperatures on the $H_2O$ side and the $sCO_2$ side. During the first 20 min, the $sCO_2$-DHRS is ramped up from its operational readiness state to full power. This can be observed from the increase of the $H_2O$ outlet and the $sCO_2$ inlet temperature of the CHX.

All parameters on the $H_2O$ side are influenced by the cyclic blow-off behaviour of the safety valves. The safety valves open at 8.83 MPa and close when the pressure drops below 8.33 MPa. Subsequently, the pressure starts to increase, rapidly at first and then slower. In Figure 6, this can be observed from the $H_2O$ inlet temperature of the CHX, which follows the behaviour of the pressure. At the start of the accident, the frequency of the blow-off is high and then decreases together with the declining decay heat. During the phase of pressure build-up, the steam enters the $H_2O$ inlet superheated from hot structures on top of the steam generator, by approximately 4 K on average. When the safety valve opens, this results in an inlet pressure and temperature drop of around 1 MPa and 10 K. In the beginning, the temperature drop is twice as high. The outlet temperature of the CHX experiences higher drops of up to 30 K but comes back to its


DOI: 10.17185/duepublico/77260

initial level considerably faster within 10 s. This behaviour is mainly related to the mass flow rate which also exhibits very short peaks related to the distribution of the natural circulation-driven flow on the $H_2O$ side. The control of the $H_2O$ outlet temperature reacts hardly, varying the relative opening area of the valve by just 3 %. This is a result of the chosen small proportional and integral gain and the omission of the derivative gain to avoid a negative interaction of the controllers.

On the $sCO_2$ side, the $sCO_2$ outlet temperature of the CHX closely follows the behaviour of the $H_2O$ inlet temperature, just shifted by approximately 15 K with exception of the ramp-up phase. The changes are within the same magnitude of 10 K, also at the following turbine outlet and UHS inlet. At the compressor inlet, the changes are reduced to less than 0.5 K by the thermal inertia of the UHS and the control of the compressor inlet temperature. The related variations of the pressures on the $sCO_2$ side are approximately 1 bar or less. The related cycle mass flow rate exhibits small peaks of approximately 0.8 kg/s magnitude or less. In the future, it should be analysed in more detail, if the cyclic thermal load poses a problem for the integrity of the components.

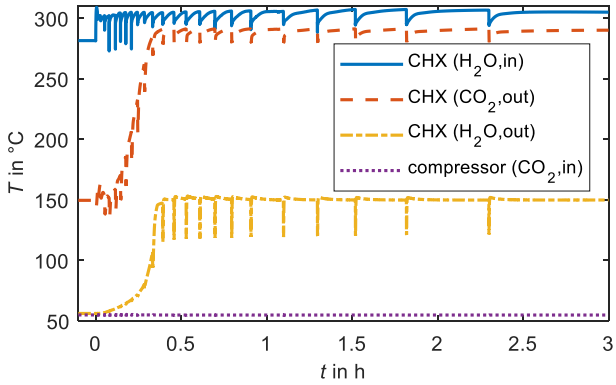


**Figure 6:** Steam generator blowdown via the safety valves: Temperatures of steam generator 1 ($H_2O$ side) and cycle 1 ($sCO_2$ side)

## VALVE FAILURE IN THE CONDENSATE LINE

In this chapter, the failure of the $H_2O$ CHX outlet temperature control is discussed. Normally, this control adapts the valve opening in the pipe after the CHX (Figure 1) to adjust the $H_2O$ mass flow rate and thereby the $H_2O$ outlet temperature with the intention to reduce the maximum temperature difference between the fluids in the CHX. The extreme cases of a control failure are a completely opened or closed valve. Opening the valve completely leads to an increase in the CHX $H_2O$ outlet temperature. The increase depends on the pressure drop in the pipes on the $H_2O$ side and the opened valve and the current water level in the steam generator. The outlet temperature may even increase to the level of the inlet temperature with condensation occurring over the whole length of the CHX. This would enable a higher heat removal from the NPP due to the increased heat transfer coefficient on the $H_2O$ side. However, also the thermal stress in the CHX increases due to a higher temperature difference between the fluids. If the applied CHX can bear high thermal stresses, the outlet temperature control may not be required except for the operational readiness state and the start-up. Moreover, a smaller CHX could be designed due to better heat transfer. If the CHX is not designed to bear high temperature differences, the valve opening can still be adjusted manually in case of a defect in the control system because this control generally acts very slowly.

If a failure of the control leads to a closed valve at the CHX outlet, this almost immediately stops the heat input to the corresponding $sCO_2$ cycle. Simulations with a considerably high decay heat curve were conducted to illustrate this fact.

In the first simulation, it was arbitrarily assumed that the valve after the CHX on the $H_2O$ side closes suddenly, 2 h after the start of the accident. Closing this valve stops the steam flow completely. As a result, the turbine inlet temperature on the $sCO_2$ side decreases steeply, which activates the shaft speed control. Since the target of the control is to keep the turbine inlet temperature constant at 260 °C, the shaft speed also decreases rapidly. Within 25 s, the shaft speed and the thermal power transfer in the CHX have already decreased to zero. The fast temperature changes might lead to high thermal stresses, which should be analysed further. If no restart of the shutdown $sCO_2$ cycle is considered, the primary and secondary loops of the NPP heat up since the decay heat is higher than the heat removal capacity of the $sCO_2$ cycles. In the primary loop, about 8 % of the total mass inventory is blown off before the primary side starts to cool down again as the equilibrium of the decay power and the total thermal power of the cycles is reached. Since no issues related to the boron concentration are observed, this simulation can be seen as an additional example of a successfully handled accident sequence even after the failure of one $sCO_2$ cycle.

A further simulation analysed the restart of the $sCO_2$ cycle assuming that the issue with the closed valve could be solved quickly. Figure 7 shows different parameters during the shutdown and following start-up procedure with the closing of the valve shifted to 0 s. On the top left, the shaft speed relative to its design speed and the relative valve opening area are displayed to illustrate the described procedure. The closing of the valve and the resulting shutdown have already been described together with the previous case. Thereafter, the valve was kept closed for 5 min and then opened to its opening area during the operational readiness state. From this point, the valve opening and the turbomachinery speed were increased linearly within 20 min until the design speed was reached again. After the ramp-up procedure, the valve opening area is controlled again to keep the CHX outlet temperature at the $H_2O$ side at its target value of 150 °C. On the top right of Figure 7, the mass flow rates of $sCO_2$ and $H_2O$ are provided at the compressor inlet and the CHX inlet, respectively. The $H_2O$ mass flow rate stays at zero while the valve is closed. After the reopening of the valve, it increases to about 0.5 kg/s and then gradually increases together with the $sCO_2$ mass flow rate. While the valve is closed, a reverse flow through the $sCO_2$ compressor can be observed which peaks shortly after the shutdown and then decreases towards zero. On


DOI: 10.17185/duepublico/77260

the bottom left, the compressor and turbine inlet temperatures are shown. The turbine inlet temperature drops steeply to 137 °C within 25 s. After the shutdown, the turbine inlet temperature decreases further down to a minimum value of 61 °C and then increases to 85 °C again because the flow in the cycle has almost reduced to zero. The compressor inlet temperature always remains close to its target value of 55 °C. After the restart, the turbine inlet temperature increased to a higher value due to the heat-up of the corresponding steam generator. In the bottom right of Figure 7, the thermal power of the CHX is displayed. The slightly higher value after the restart compared to before the shutdown is also related to the higher temperatures on the $H_2O$ side. Even without opening the compressor recirculation and the turbine bypass, the compressor operation keeps a sufficient margin to the surge line during the whole procedure. This is related to the already increased turbine inlet temperature at the start of the restart procedure. In the future, it should be investigated further under which conditions a restart can be conducted.

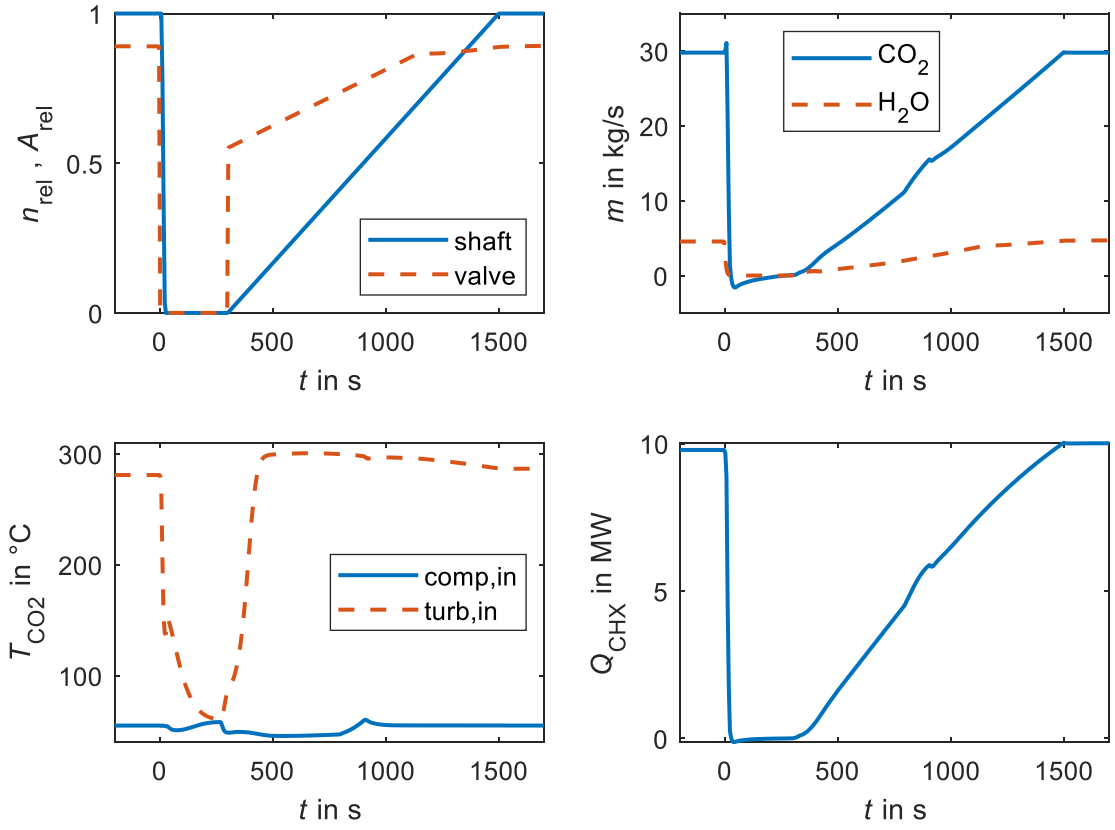


**Figure 7:** Unintended closing of the valve at CHX $H_2O$ outlet and reopening 5 min later: various parameters during the shutdown and restart of the related $CO_2$ cycle

## CONCLUSION

In this study, different sudden failures during the operation of the $sCO_2$-DHRS were analysed with the thermal-hydraulic system code ATHLET. The system was coupled to a generic Konvoi PWR with a thermal power of 3840 MW and conservative boundary conditions were applied with regard to ambient temperature and decay heat during a combined long-term station blackout and loss of the ultimate heat sink scenario.

The results, which are summarized in Table 1, show that the applied design of the $sCO_2$-DHRS, which was presented in previous studies, can cope with some of the assumed events but other cases either require fast intervention or further design or control improvements. In most cases, the failure of a single $sCO_2$ cycle can be compensated, either by the control of the cycles and the thermal inertia of the PWR or by losing some inventory in case of an early failure. However, additional backup cycles should be installed to cover the unavailability of one or multiple cycles in case of a very early failure or maintenance. On the one hand, failure of the fans of the gas cooler leads to a pressure increase which may be mitigated by an inventory control system or the shutdown of the respective cycle. On the other hand, unintended fan speed-up can cause compressor surge or a drop of the cycle pressure into the two-phase region. This requires a fast intervention, e.g. preventing or stopping and reverting the speed-up within a couple of seconds. Moreover, the $sCO_2$-DHRS can operate under the cyclic blow-off from the steam generator


DOI: 10.17185/duepublico/77260

safety valves when the relief valves are not available. Finally, the unintended closure of the valve which controls the steam flow through the CHX triggers a fast cycle shutdown but a subsequent restart might be possible.

In the future, it may be investigated further under which conditions and how a restart can be conducted. Furthermore, it should be analysed in detail if thermal stresses caused by high thermal gradients or high temperature differences can cause damage to the components. This is also related to the analysis of the necessity of the control of the CHX outlet temperature on the $H_2O$ side. For highly transient cases, not only the thermal inertia of the heat exchangers but also of the pipe walls and the material of the turbomachinery should be modelled. Moreover, the mechanical inertia of the turbomachinery should be considered. Finally, advanced control strategies may help to reduce thermal stresses and enable adequate countermeasures in various failure scenarios.

**Table 1:** Summary of analysed failures: Impact and possible measures

| Failure name | Impact | Measures |
|---|---|---|
| Failure of (single) $sCO_2$ cycle | All except early failures can be compensated | Back-up cycles for early or multiple cycle failures |
| Fan failure (loss of cooling) | Decreased heat removal capacity; high cycle pressures | See previous; inventory control system, intentional shutdown |
| Unintended fan speed-up | Fast decrease of cycle temperatures and pressures; compressor surge | Stop/limit fan speed increase; opening of bypass/ recirculation |
| Cyclic blow-off from the steam generator safety valves | Cyclic thermal load, partially cyclic behaviour of cycle parameters | Integrity check of components (thermo-mechanical analysis) |
| Valve failure in the condensate line (completely open valve) | Increased heat removal, temperatures and temperature differences | Integrity check of CHX; if positive: option for higher heat removal/ smaller CHX design |
| Valve failure in the condensate line (completely closed valve) | Stop of heat removal of corresponding cycle, cycle shutdown | Cycle restart after the issue is solved, backup cycles |

## NOMENCLATURE

| | |
|---|---|
| $A$ | opening area of the valve (m²) |
| $m$ | mass flow rate (kg/s) |
| $n$ | rotational speed (krpm) |
| $p$ | pressure (MPa) |
| $t$ | time (h) |
| $T$ | temperature (°C) |
| $Q$ | thermal power (MW) |

*Subscripts*

| | |
|---|---|
| comp | compressor |
| in | inlet |
| out | outlet |
| rel | relative |
| turb | turbine |

*Acronyms*

| | |
|---|---|
| CHX | compact heat exchanger |
| CL | cold leg |
| DHRS | decay heat removal system |
| FWL | feed water line |
| $H_2O$ | water |
| HL | hot leg |
| LCQ | steam generator blowdown system |
| MSL | main steam line |
| NPP | nuclear power plant |
| PRZ | pressurizer |
| RPV | reactor pressure vessel |
| PWR | pressurized water reactor |
| $sCO_2$ | supercritical carbon dioxide |
| SG | steam generator |
| TAC | turbomachinery (turbo-alternator-compressor) |
| UHS | gas cooler/ heat exchanger to the diverse ultimate heat sink (ambient air) |


## ACKNOWLEDGEMENTS

The research presented in this paper has received funding from the Euratom research and training programme 2014-2018 under grant agreement No. 847606 “Innovative sCO2-based Heat removal Technology for an Increased Level of Safety of Nuclear Power plants” (sCO2-4-NPP).

The work of University of Stuttgart was also funded by the German Ministry for Economic Affairs and Energy (BMWi. Project No. 1501557) on basis of a decision by the German Bundestag


## REFERENCES


[1] White, M.T., Bianchi, G., Chai, L., Tassou, S.A. and Sayma, A.I. (2021) Review of supercritical CO2 technologies and systems for power generation. *Applied Thermal Engineering*, 185. https://doi.org/10.1016/j.applthermaleng.2020.116447

[2] Wu, P., Ma, Y., Gao, C., Liu, W., Shan, J., Huang, Y. et al. (2020) A review of research and development of supercritical carbon dioxide Brayton cycle technology in nuclear engineering applications. *Nuclear Engineering and Design*, Elsevier. 368, 110767. https://doi.org/10.1016/j.nucengdes.2020.110767

[3] D’Auria, F. (2017) Thermal-Hydraulics of Water Cooled Nuclear Reactors. Elsevier.



DOI: 10.17185/duepublico/77260

https://doi.org/10.1016/C2015-0-00235-0

[4] Bestion, D. (2008) System code models and capabilities. *THICKET*, Grenoble. p. 81–106.

[5] Wu, P., Gao, C. and Shan, J. (2018) Development and Verification of a Transient Analysis Tool for Reactor System Using Supercritical $CO_2$ Brayton Cycle as Power Conversion System. *Science and Technology of Nuclear Installations*, Hindawi. 2018, 1–14. https://doi.org/10.1155/2018/6801736

[6] Wang, H., Sun, L., Wang, H., Shi, L. and Zhang, Z. (2013) Dynamic Analysis of S-CO2 Cycle Control With Coupled PDC-SAS4A/SASSYS-1 Codes. *International Conference on Nuclear Engineering, Proceedings, ICONE*, American Society of Mechanical Engineers Digital Collection. 2, 633–40. https://doi.org/10.1115/ICONE20-POWER2012-54547

[7] Venker, J. (2015) Development and Validation of Models for Simulation of Supercritical Carbon Dioxide Brayton Cycles and Application to Self-Propelling Heat Removal Systems in Boiling Water Reactors. Stuttgart. https://doi.org/10.18419/opus-2364

[8] Mauger, G., Tauveron, N., Bentivoglio, F. and Ruby, A. (2019) On the dynamic modeling of Brayton cycle power conversion systems with the CATHARE-3 code. *Energy*, Elsevier Ltd. 168, 1002–16. https://doi.org/10.1016/j.energy.2018.11.063

[9] Batet, L., Alvarez-Fernandez, J.M., Mas de les Valls, E., Martinez-Quiroga, V., Perez, M., Reventos, F. et al. (2014) Modelling of a supercritical $CO_2$ power cycle for nuclear fusion reactors using RELAP5–3D. *Fusion Engineering and Design*, North-Holland. 89, 354–9. https://doi.org/10.1016/J.FUSENGDES.2014.03.018

[10] Hexemer, M. and Rahmer, K. (2011) Supercritical CO2 Brayton Cycle Integrated System Test (IST) TRACE Model and Control System Design. *Supercritical CO2 Power Cycle Symposium*, Boulder, Colorado. p. 1–58.

[11] Hofer, M., Buck, M. and Starflinger, J. (2019) ATHLET extensions for the simulation of supercritical carbon dioxide driven power cycles. *Kerntechnik*, 84, 390–6. https://doi.org/10.3139/124.190075

[12] Hofer, M., Buck, M., Cagnac, A., Prusek, T., Sobecki, N., Vlcek, P. et al. (2020) Deliverable 1.2: Report on the validation status of codes and models for simulation of sCO2-HeRo loop. sCO2-4-NPP.

[13] Hofer, M., Theologou, K. and Starflinger, J. (2021) Qualifizierung von Analysewerkzeugen zur Bewertung nachwärmegetriebener, autarker Systeme zur Nachwärmeabfuhr – sCO2-QA -. Stuttgart.

[14] Austregesilo, H., Bals, C., Hora, A., Lerchl, G., Romstedt, P., Schöffel, P. et al. (2016) ATHLET Models and Methods. Garching.

[15] Gesellschaft für Anlagen- und Reaktorsicherheit gGmbH. (2019) ATHLET. https://user-codes.grs.de/athlet

[16] Hofer, M., Ren, H., Hecker, F., Buck, M., Brillert, D. and Starflinger, J. (2022) Simulation, analysis and control of a self-propelling heat removal system using supercritical CO2 under varying boundary conditions. *Energy*, Pergamon. 123500. https://doi.org/10.1016/J.ENERGY.2022.123500

[17] Hajek, P., Vojacek, A. and Hakl, V. (2018) Supercritical $CO_2$ Heat Removal System - Integration into the European PWR fleet. *2nd European SCO2 Conference*, Essen. p. 0–7. https://doi.org/10.17185/duepublico/460

[18] Vojacek, A., Hakl, V., Hajek, P., Havlin, J. and Zdenek, H. (2016) Deliverable 1.3: Documentation system integration into European PWR fleet. sCO2-HeRo.

[19] Pham, H.S., Alpy, N., Ferrasse, J.H., Boutin, O., Tothill, M., Quenaut, J. et al. (2016) An approach for establishing the performance maps of the sc-CO2 compressor: Development and qualification by means of CFD simulations. *International Journal of Heat and Fluid Flow*, 61, 379–94. https://doi.org/10.1016/j.ijheatfluidflow.2016.05.017

[20] Hofer, M., Buck, M. and Starflinger, J. (2021) OPERATIONAL ANALYSIS OF A SELF-PROPELLING HEAT REMOVAL SYSTEM USING SUPERCRITICAL CO2 WITH ATHLET. *4th European SCO2 Conference*, online. p. 1–11. https://doi.org/10.17185/DUEPUBLICO/73983

[21] Hofer, M., Ren, H., Hecker, F., Buck, M., Brillert, D. and Starflinger, J. (2021) Simulation and analysis of a self-propelling heat removal system using supercritical CO2 at different ambient temperatures. *4th European Supercritical CO2 Conference*, online. p. 1–14. https://doi.org/10.17185/DUEPUBLICO/73943

[22] Ren, H., Hacks, A., Schuster, S. and Brillert, D. (2021) Mean-line analysis for supercritical CO2 centrifugal compressors by using enthalpy loss coefficients. *4th European Supercritical CO2 Conference*, online. https://doi.org/10.17185/duepublico/73948

[23] Frýbort, O., Kriz, D., Melichar, T., Vlcek, P., Hakl, V., Vyskocil, L. et al. (2021) Deliverable 5.4: Thermodynamic performance of the heat recovery system integrated into the plant. sCO2-4-NPP.

[24] Hofer, M., Buck, M., Prusek, T., Sobecki, N., Vlcek, P., Kriz, D. et al. (2021) Deliverable 2.2: Analysis of the performance of the sCO2-4-NPP system under accident scenarios based on scaled-up components data. sCO2-4-NPP.

[25] Sobecki, N., Delmaere, T., Hofer, M. and Vlcek, P. (2022) Deliverable 5.5: Integration of data from real design parameters into the thermal-hydraulic code and simulations based on accident scenarios. sCO2-4-NPP.

[26] Hexemer, M.J., Hoang, H.T., Rahner, K.D., Siebert, B.W. and Wahl, G.D. (2009) Integrated Systems Test (IST) Brayton Loop Transient Model Description and Initial Results. *S-CO2 Power Cycle Symposium*, Troy. p. 1–172.

[27] Carstens and Nathan. (2007) Control strategies for supercritical carbon dioxide power conversion systems. *Massachusetts Institute of Technology*,.

 DOI: 10.17185/duepublico/77260

[28] Moisseytsev, A. and Sienicki, J.J. (2016) SIMULATION OF S-CO2 INTEGRATED SYSTEM TEST WITH ANL PLANT DYNAMICS CODE. *The 5 Th International Symposium-Supercritical CO2 Power Cycles*, San Antonio.

[29] Moisseytsev, A. and Sienicki, J.J. (2019) Analysis of thermal transients for SCO2 Brayton cycle heat exchangers. *Proceedings of the ASME Turbo Expo*, 9, 1–12. https://doi.org/10.1115/GT2019-90374

[30] Wang, R., Li, X., Qin, Z., Wang, L., Lin, Z., Wang, X. et al. (2022) Dynamic response and emergency measures under failure conditions of sCO 2 Brayton cycle. https://doi.org/10.1002/ese3.1300


DOI: 10.17185/duepublico/77260

**DOI:** 10.17185/duepublico/77260
**URN:** urn:nbn:de:hbz:465-20230427-094259-3